Asynchronous learning-based output feedback sliding mode control for semi-Markov jump systems: a descriptor approach

Zheng Wu, Yiyun Zhao, Fanbiao Li, *Senior Member, IEEE*, Tao Yang, *Senior Member, IEEE*, Yang Shi, *Fellow, IEEE*, Weihua Gui, *Member, IEEE*

***Abstract*—This paper presents an asynchronous output-feedback control strategy of semi-Markovian systems via sliding mode-based learning technique. Compare with most literature results that require exact prior knowledge of system state and mode information, an asynchronous output-feedback sliding surface is adopted in the case of incompletely available state and non-synchronization phenomenon. The holonomic dynamics of the sliding mode are characterized by a descriptor system in which the switching surface is regarded as the fast subsystem and the system dynamics are viewed as the slow subsystem. Based upon the co-occurrence of two subsystems, the sufficient stochastic admissibility criterion of the holonomic dynamics is derived by utilizing the characteristics of cumulative distribution functions. Furthermore, a recursive learning controller is formulated to guarantee the reachability of the sliding manifold and realize the chattering reduction of the asynchronous switching and sliding motion. Finally, the proposed theoretical method are substantiated through two numerical simulations with the practical continuous stirred tank reactor and F-404 aircraft engine model.**

***Index Terms*—Sliding mode control, semi-Markovian jump systems, output feedback, learning-based control, asynchronous switching.**

I. Introduction

Sliding mode control (SMC) has attracted considerable attention due to its fast response and insensitivity to perturbation [1]–[4]. The key design of the SMC lies in the construction of a suitably-defined hyper-surface and a surface-dependent controller such that the state trajectories can be steered onto the specific sliding surface (called the approaching phase) and remain it thereafter (called the sliding phase). A common fact in these SMC strategy is the availability of full states information, and such control strategy has limitations in practical implementation since the state information may not be fully accessible in real time. Therefore, output-based feedback sliding mode approach is of more practice (see, e.g., [5]–[8] and references therein included). Furthermore, in the traditional SMC, there exists nonnegligible chattering phenomenon and oscillations in the vicinity of the sliding surface caused by the discontinuity of symbolic function [9]. In order to improve the control accuracy and smoothness for SMC systems, some profound works on the smooth transition performance are shown in [10]–[16]. Specifically, by means of solving Function-Harmonic Balance equation, the quantitative analysis of chattering amplitude for high order SMC has been analyzed from the perspective of frequency domain in [14]. In [15], a new actuator fault estimation scheme is developed for linear systems based on sliding mode observer method by using quantized measurements. To mitigate the conservatism of large gains, [16] proposes a framework combining switching and variable gain methods for chattering attenuation via hybrid variation construction of SMC controller parameters.

To tackle the issue of chattering, a sliding mode-based learning control (SMLC) method has been reported in literature [17]–[19]. Rather than adopting discontinuous step term, the error direction information and activating control in SMLC depend are to design iterative learning transition term. The improved learning term, which is based on the approximation of the gradient of the Lyapunov function, can modify the control signal to guarantee the smooth reachability of sliding mode trajectory. As stated in [20], the SMLC is not only an efficient method against external disturbances as SMC, but also has a lower computational complexity than recursive-learning controller. In this article, the output SMLC design problem is addressed where reachability during the convergence phase and stability during the sliding phase are investigated. Exploring a more complicated and practical control framework to unsolved output SMLC problems is the primary concern and first motivation of this study.

In another research field, Markov jump systems (MJSs) have superior features in characterizing complex physical systems with multi-mode switching dynamics [21]–[24]. Over the past few decades, extensive research on MJSs have been established in theoretical investigation and engineering exploration [25]–[27]. Nonetheless, the inherent memoryless characteristic of the Markov chain imposes limitations on broader applications. This is due to the fact that the probability density

This work was supported in part by the National Science Fund for Excellent Young Scholars of China under Grant 62222317; in part by the National Science Foundation of China under Grant 62303492; in part by the Major Science and Technology Projects in Hunan Province 2021GK1030; in part by the Science and Technology Innovation Program of Hunan Province 2022WZ1001; in part by the Key Research and Development Program of Hunan Province under Grant 2023GK2023; in part by the Fundamental Research Funds for the Central Universities of Central South University 2024ZZTS0116. *(Corresponding author: Yiyun Zhao.)*

Z. Wu, Y. Zhao, F. Li, and W. Gui are with the School of Automation, Central South University, Changsha, 410083, China. (e-Mail:wuzheng@csu.edu.cn; yiyun.felix.zhao@gmail.com; fanbiaoli@csu.edu.cn; gwh@csu.edu.cn).

Tao Yang is with the Power Electronics, Machines and Control Group, The University of Nottingham, Nottingham NG7 2RD, U.K. (emails: Tao.Yang@nottingham.ac.uk).

Y. Shi is with the Department of Mechanical Engineering, University of Victoria, Victoria, BC V8W 3P6, Canada. (e-mail:yshi@uvic.ca).

function of the duration between consecutive mode switches conforms to the exponential and geometrical distribution in the continuous- and discrete-time domains. It should be emphasized that time-invariant transfer probabilities is inadequate to characterise some real stochastic systems, such as the degradation processes of heterogeneous fleets, the population ecological systems and among others [28]–[31]. To relax such a restriction, the semi-Markov jump systems (SMJSs) have been put forward as a natural generalization of MJSs. The transition rates or probabilities of the semi-Markov process are time-nonhomogeneous in the continuous- or discrete-time cases and its sojourn-time subject to an arbitrary probability distribution. Consequently, SMJSs provide a more generalized and comprehensive description for the systems with stochastic switching [32]–[34]. The robust stochastic stabilization analysis and controller design approach therein follow from dissecting the infinitesimal operators under time-varying transfer probabilities [32], which require the upper and lower bound information of a probability density function. While in [33] eschews this prior information necessity, the mean square stability and stabilization of SMJSs have been studied via a quantitative analysis approximation to the length of sojourn-time.

Nevertheless, the aforementioned works leave some room for the improvement of multi-mode stochastic switched systems with SMC strategy, because there are two implicit assumption that the accurate system mode signal is accessible instantaneously for the SMC controller design and the SMC operational mode should be switched synchronously with the obtained mode. Note, such premises are stringent in practice for the following two layers of reasons. First, the delay of signal transmission or the disorder of data packets will affect the instantaneity and accuracy of the controller to obtain the random switching signal of the system. Second, it is hard for the controller to switch its operation mode in time under the given system mode signal due to the limitation of the implementation of the intermediate actuator. In other words, the asynchronous switching phenomenon is unavoidable in the stochastic switched systems with multi-mode controller in practical applications. In the light of this, hidden Markov process has been presented to realize the asynchronous control when the real system mode is indirectly accessible for the controller [35]. The hidden Markov chains is constituted as a dual-layer parametric process. The bottom layer is a stochastic process that is characterized as a finite-state Markov chain, in which the system modes are not accessible to controllers/observers directly. The upper layer is an observed mode sequence that is related to the underlying stochastic process. To better characterize the asynchronization phenomenon and enhance resilience against perturbations for the SMJSs with doubly-stochastic process, a novel SMC framework with prior statistical probability information, that is, asynchronous SMLC, is appealing to be comprehensively investigated to alleviate the shortcomings of existing methods, which is the second and major inspiration of this paper.

Inspired by the above theoretical and technical discussion, in this paper, a stabilization criterion for the holonomic SMD is provided on the basis of descriptor approach, and the asynchronous sliding mode-based learning control law of continuous-time SMJSs is constructed to guarantee the reaching of the sliding manifold. The main contributions of the paper are threefold:

i) Considering the influence of complex operating environment and signal transmission constraints, two rigorous assumptions, i.e., the sojourn time in stochastic switched systems obeys the exponential distribution, the mode switching of the system and controller is synchronized, are removed in this paper by applying the semi-Markov chain and prior statistical probability information.
ii) To avoid undesired oscillations induced by the discontinuous switching term, this paper introduces a novel sliding mode-based learning controller combined with an asynchronous switching mechanism and the corresponding stochastic admissibility (SA) criterion of the sliding behavior is obtained via the descriptor approach.
iii) Different from previous SMC methods requiring full available state information in [17], the output information is incorporated to establish the sliding surface of which attainability can be obtained by proposed SMLC law within a finite time interval, and the SMLC law ensures that the system trajectory can be driven onto the sliding surface within a finite time interval, greatly enhancing the feasibility without resorting to full system state information.

Notations. $\mathbb{R}_+$ is the set of non-negative real numbers. $\mathbb{R}_{[\varsigma_1,\varsigma_2]}$ indicates $\{\varepsilon \in \mathbb{R} \mid \varsigma_1 \leqslant \varepsilon \leqslant \varsigma_2\}$. $\overline{\varsigma_1,\varsigma_2}$ represents consecutive positive integer subset $\{\varsigma_1, \varsigma_1+1, \cdots, \varsigma_2\}$. $\mathbb{E}$ is the mathematical expectation. $\mathcal{L}$ denotes the weak infinitesimal operator. $\mathrm{Span}(X)$ denotes the subspace spanned by the vectors in X. The transpose of the matrix X in denoted by $X^\top$.

II. Problem Statement

A class of continuous-time SMJSs with parameters $\{r_t\}_{t\in\mathbb{R}_+}$ defined on a probability space $\{\Omega, \mathcal{F}, \mathrm{Pr}\}$ are considered as follows:

$$\begin{cases} \dot{x}(t) = A(r_t)x(t) + B(r_t)\left[u(t) + f(t, x(t))\right], \\ y(t) = C(r_t)x(t), \end{cases} \tag{1}$$

where $x(t) \in \mathbb{R}^m$, $u(t) \in \mathbb{R}^n$ are the state and control input variables, respectively. $f(t, x(t)) \in \mathbb{R}^n$, $y(t) \in \mathbb{R}^p$ denote the nonlinear perturbation function and output variables, respectively. The matrices $A(r_t)$, $B(r_t)$ and $C(r_t)$ are real known matrices and adhere to dimension compatibility principle. $B(r_t)$ and $C(r_t)B(r_t)$ satisfy the full of column rank.

The undermentioned concepts and definitions are given to better describe semi-Markov chain. The stochastic process $\{(R_k, t_k)\}$ is a homogeneous Markov renewal process with a embedded Markov chain $\{R_k\}$ and the kth transition instant t_k. The values of the Markov process $\{R_k\}$ are all within the set $\mathcal{M} = \overline{1, M}$ and its transition probability from mode i to mode j for $i, j \in \mathcal{M}$ is given by $q_{ij} := \mathrm{Pr}\{r_{k+1} = j \mid r_k = i\}$. Denote $N_t = \sup\{k : t_k \leqslant t\}$, $\{r_t\}$ can be regarded as a semi-Markov process associated with the renewal process

$\{(R_k, t_k)\}$ when $r_t = R_{N_t}$ (more details can refer to [33], [36]). The stochastic process $\{T_k\}$ indicates the time interval between the $(k-1)$th and kth jumps, $T_k := t_k - t_{k-1}$. In addition, $g_i(h)$ is the probability density function and $G_i(h)$ is the cumulative distribution function of sojourn-time h residing in mode i, i.e., $G_i(h) = \Pr\{T_{k+1} < h | r_{t_k} = i\}$.

It should be noted that stochastic process $\{r_t\}$ differs from $\{R_k\}$. The time parameter of semi-Markov process $\{r_t\}$ is t while embedded Markov chain $\{R_k\}$ is jump instant t_k. The transition rate matrix $\Theta(h) = [\theta_{ij}(h)]_{M\times M}$ between two successive modes is given by

$$\begin{aligned}&\Pr\{r_{t+\Delta} = j | r_t = i\}\\ &= \begin{cases} \Pr\{T_{k+1} \leqslant h+\Delta, R_{k+1} = j \mid T_{k+1} > h, R_k = i\} \\ \qquad = \theta_{ij}(h)\Delta + o(\Delta) \qquad \text{if} \quad i \neq j, \\ \Pr\{T_{k+1} > h+\Delta \mid T_{k+1} > h, R_k = i\} \\ \qquad = 1 + \theta_{ii}(h)\Delta + o(\Delta) \quad \text{if} \quad i = j, \end{cases}\end{aligned} \tag{2}$$

where $\Delta > 0$ and $\lim_{\Delta\to 0} o(\Delta)/\Delta = 0$; $\theta_{ij}(h) \geqslant 0, j \neq i$ and $\theta_{ii}(h) = -\sum_{j\neq i, j\in\mathcal{M}} \theta_{ij}(h)$ for all $i \in \mathcal{M}$. For the mode transition process of SMJSs (1), the following structure holds

$$\lambda_{ij}(h) = q_{ij}\frac{g_i(h)}{1 - G_i(h)}, \tag{3}$$

for $(i,j) \in \mathcal{M}\times\mathcal{M}$, $i \neq j$. Moreover, $\bar{\theta}_{ij} := \mathbb{E}\{\theta_{ij}(h)\} = \int_0^\infty \theta_{ij}(\nu)g_i(\nu)\,\mathrm{d}\nu$. For brevity, the matrices $A(r_t)$, $B(r_t)$ and $C(r_t)$ are denoted by A_i, B_i and C_i, for $r_t = i \in \mathcal{M}$.

Control objective: The purpose of this paper is to design an asynchronous output sliding surface based on singular systems theory such that the sliding mode dynamics is stochastic admissibility, and then synthesize an iterative learning sliding mode control law such that the closed-loop system trajectories can be steered onto the predefined sliding surface.

III. Main Results

To begin with, the asynchronous output feedback sliding surface will be synthesized and the corresponding SA of the holonomic sliding mode dynamics (SMD) is derived from different time scale. Then, a learning-based sliding mode controller is put forward under which the state trajectory of the global system can reach to the pre-desired sliding mainfold.

In order to characterize the asynchronous phenomenon, a stochastic process σ_t, in which the values lie in a finite space $\mathcal{N} = \overline{1,N}$, is assigned to denote the controller mode and associated with r_t via the emission probability matrix $\Upsilon = [\vartheta_{i\phi}]$:

$$\Pr(\sigma_t = \phi \mid r_t = i) = \vartheta_{i\phi}, \tag{4}$$

where $\vartheta_{i\phi} \in \mathbb{R}_{[0,1]}$ and $\sum_{\phi\in\mathcal{N}} \vartheta_{i\phi} = 1$, $\forall i \in \mathcal{M}, \phi \in \mathcal{N}$.

Remark 1: The stochastic process $\{\sigma_t\}_{t\in\mathbb{R}_+}$ depends on the semi-Markov process $\{r_t\}_{t\in\mathbb{R}_+}$ with emission probability (4) that connects the actual plant mode and the corresponding controller mode. It is noteworthy that in SMJSs, the underlying operation mode r_t would remain as i, whereas the random variables σ_t may change during the sojourn-time $[t_k, t_{k+1})$. Therefore, the stable performance and stabilization problems of the doubly-stochastic parametric jumping systems are more complicated than that of conventional Markov or semi-Markov systems.

The following asynchronous output-based sliding function is designed for the semi-Markov jump system (1):

$$s(\phi, t) = S_\phi y(t), \tag{5}$$

where $S_\phi \in \mathbb{R}^{n\times p}, \phi \in \mathcal{N}$ are the sliding surface parameters which is demonstrated in subsequent results.

The asynchronous output-based sliding mode surface, as considered in this paper, encompasses several special cases: 1) synchronous mode-dependent switching scenario, i.e., $s(r_t, t) = S(r_t)y(t)$ when $\mathcal{N} = \mathcal{M}$, $\forall i = \phi$ and $\vartheta_{i\phi} = 1$ as discussed in [5]; 2) mode clustering scenario, i.e. $s(\hat{r}_t, t) = S(\hat{r}_t)y(t)$ when $\mathcal{M} = \bigcup_{i=1}^N M_i$ in [22], where $\hat{r}_t$ indicates the cluster to which $r(t)$ belongs; 3) single mode switching scenario, characterized by $s(t) = Sy(t)$ when $\mathcal{N} = \{1\}$.

In line with the SMC theory, the switching function conforms to $s(\phi, t) = 0$ and $\dot{s}(\phi, t) = 0$ when the system trajectory reaches the sliding manifold. $B_i^\perp \in \mathbb{R}^{(m-n)\times m}$ is one of orthonormal basis of the null space of B_i, then construct nonsingular matrices T_i for $i \in \mathcal{M}$ as follows

$$T_i = \begin{bmatrix} B_i^\perp \\ B_i^\top \end{bmatrix}. \tag{6}$$

The system (1) can be transformed with matrix T_i as:

$$T_i\dot{x}(t) = T_iA_ix(t) + T_iB_i\left[u(t) + f(t, x(t))\right], \tag{7}$$

which is reformulated as

$$\begin{cases} B_i^\perp\dot{x}(t) = B_i^\perp A_ix(t), \\ B_i^\top\dot{x}(t) = B_i^\top A_ix(t) + B_i^\top B_i\left[u(t) + f(t, x(t))\right]. \end{cases} \tag{8}$$

The SMD of the SMJS is obtained by the first equation of system (8). Together with $s(\phi, t) = 0$, the holonomic SMD can be in the form of

$$E_i\dot{x}(t) = \bar{A}_{i\phi}x(t), \tag{9}$$

where

$$E_i = \begin{bmatrix} B_i^\perp \\ 0 \end{bmatrix}, \quad \bar{A}_{i\phi} = \begin{bmatrix} B_i^\perp A_i \\ S_\phi C_i \end{bmatrix}. \tag{10}$$

Remark 2: Observing that the SMD can be comprehensively captured by the descriptor system (9), which comprises the sliding surface (5) as the fast components and the first equation in the original system (8) as slow components. Consequently, ensuring the stochastic admissibility of the descriptor system (9) can achieve the attainment of the specified sliding surface (5).

Remark 3: If the mode-dependent input coefficient matrix B_i with full column rank satisfying that $\mathrm{Span}(B_1) = \mathrm{Span}(B_2) = \cdots = \mathrm{Span}(B_M)$, then there exists a full row rank matrix $Q \in \mathbb{R}^{(m-n)\times m}$ such that $QB_i = 0$. Accordingly, the transformation matrix T_i can be chosen as $\begin{bmatrix} Q^\top & B_i \end{bmatrix}^\top$. Subsequently, the SMD with E_i is replaced by E, which is fixed and in a continuous-time domain. However, such a premise is generally not satisfied, so the transformation matrix T_i is heterogeneous in different system modes. As a result, matrix E_i is mode-dependent and different from the fixed matrix E in most previous Markov or semi-Markov singular systems.

Since the asynchronous phenomenon occurs inevitably in practice, the transition probability (4) has been introduced to associate the system modes and controller modes. Thus, the semi-Markov chain r_t and the controller mode signal σ_t constitute a doubly stochastic process and the switchover of descriptor system (9) is determined by the aforementioned hidden semi-Markov chain.

Next, we recall the definition of stochastic admissibility for the analysis of continuous-time descriptor SMJSs.

Definition 1: [38] The descriptor system (9) is said to be

1) regular, if $\det(sE_i - A_{i\phi})$, for each $i \in \mathcal{M}$, $\phi \in \mathcal{N}$, is not identically zero;
2) impulse-free, if $\deg(\det(sE_i - A_{i\phi})) = \mathrm{rank}(E_i)$ is satisfied, for each $i \in \mathcal{M}$, $\phi \in \mathcal{N}$;
3) stochastically stable, if for any $x(0) \in \mathbb{R}^n$, $r_0 \in \mathcal{M}$, there exists a finite scale $\mathcal{C}_0 \in \mathbb{R}_+$ such that:
$$\mathbb{E}\left[\int_0^\infty \|x(t)\|^2 \mathrm{d}t\right]\bigg|_{x(0),r_0} \leqslant \mathcal{C}_0;$$
4) The descriptor system (9) is said to be stochastically admissible, if it meets 1), 2) and 3).

As a consequence, the corollary below provides stochastically admissibility condition and numerically solvable parameterization of sliding surface in (5) for the singular hidden semi-Markov jump system (9).

Theorem 1: Consider the SMJS (1) and sliding function (5), then the SMD (9) is stochastically admissible, if the symmetric matrices $P_{1i} > 0$, matrices $W_{i\phi}$, V_ϕ, U_ϕ, $\forall i \in \mathcal{M}$, $\phi \in \mathcal{N}$ with given scalar $\mu > 0$ such that the following conditions are satisfied
$$\begin{aligned}&A_i^\top(B_i^\perp)^\top P_{11i}B_i^\perp + (B_i^\perp)^\top P_{11i}B_i^\perp A_i\\&+\textstyle\sum_{i\in\mathcal{M}}\bar{\theta}_{ij}(B_j^\perp)^\top P_{11j}B_j^\perp + \textstyle\sum_{\phi\in\mathcal{N}}\vartheta_{i\phi}W_{i\phi} < 0,\end{aligned} \quad (11)$$
$$\begin{bmatrix}\Psi_{1i\phi} & \Psi_{2i\phi}\\ * & -\mu(V_\phi + V_\phi^\top)\end{bmatrix} < 0, \quad (12)$$
where $\Psi_{1i\phi} = B_iU_\phi C_i + C_i^\top U_\phi^\top B_i^\top - W_{i\phi}$, $\Psi_{2i\phi} = [(B_i^\perp)^\top H^\top + B_i]P_{22i} - B_iV_\phi + \mu C_i^\top U_\phi^\top$, and
$$H = \begin{cases}\begin{bmatrix}I & 0_{(n-m)\times(2m-n)}\end{bmatrix}^\top, & \text{if} \quad n < 2m,\\ \begin{bmatrix}I & 0_{m\times(n-2m)}\end{bmatrix}, & \text{if} \quad n \geqslant 2m.\end{cases} \quad (13)$$
Moreover, the sliding surface parametric matrices are given by $S_\phi = V_\phi^{-1}U_\phi$.

Proof: To analyze the SA of the descriptor SMJS (9), choose a Lyapunov functional candidate as
$$V_1(x(t), r_t, \sigma_t, t) = x^\top(t)E^\top(r_t)P(r_t)x(t). \quad (14)$$
The proof procedure can be divided into the following three steps.

1) The the following inequalities hold if the conditions in (11) and (12) are satisfied
$$\sum_{\phi\in\mathcal{N}}\vartheta_{i\phi}(P_i^\top\bar{A}_{i\phi} + \bar{A}_{i\phi}^\top P_i) + \sum_{j\in\mathcal{M}}\bar{\theta}_{ij}E_j^\top P_j < 0, \quad (15)$$
$$E_i^\top P_i = P_i^\top E_i > 0. \quad (16)$$

Decomposing the Lyapunov matrix P_i to conform the block in the matrices $\bar{A}_{i\phi}$ and E_i:
$$P_i = \begin{bmatrix}P_{11i} & P_{12i}\\ P_{21i} & P_{22i}\end{bmatrix}T_i, \quad (17)$$
where $P_{11i} \in \mathbb{R}^{(m-n)\times(m-n)}$, $P_{12i} \in \mathbb{R}^{(m-n)\times n}$, $P_{21i} \in \mathbb{R}^{n\times(m-n)}$, and $P_{22i} \in \mathbb{R}^{n\times n}$. Due to the symmetry of matrices $E_i^\top P_i$ in (16), it can deduce that $P_{12i} = 0$. The sliding surface parametric matrices S_ϕ are only related to the second row of the matrix $\bar{A}_{i\phi}$, matrices P_{21i} is allowed to select as $P_{22i}H$ with H given in (13). With the substitution of matrix P_i, these manipulations turn condition (15) into
$$\begin{aligned}\sum_{\phi\in\mathcal{N}}\vartheta_{i\phi}\Big(&B_iP_{22i}^\top\mathcal{S}_\phi C_i + C_i^\top\mathcal{S}_\phi^\top P_{22i}B_i^\top + C_i^\top\mathcal{S}_\phi^\top P_{22i}HB_i^\perp\\&+(B_i^\perp)^\top H^\top P_{22i}^\top\mathcal{S}_\phi C_i\Big) + A_i^\top(B_i^\perp)^\top P_{11i}B_i^\perp\\&+(B_i^\perp)^\top P_{11i}B_i^\perp A_i + \sum_{j\in\mathcal{M}}\bar{\theta}_{ij}(B_j^\perp)^\top P_{11j}B_j^\perp < 0.\end{aligned} \quad (18)$$

Following the same line of proof in [37, Lemma 5], inequality (18) can be guaranteed by the following conditions
$$\begin{aligned}&A_i^\top(B_i^\perp)^\top P_{11i}B_i^\perp + (B_i^\perp)^\top P_{11i}B_i^\perp A_i\\&+\sum_{i\in\mathcal{M}}\bar{\theta}_{ij}(B_j^\perp)^\top P_{11j}B_j^\perp + \sum_{\phi\in\mathcal{N}}\vartheta_{i\phi}W_{i\phi} < 0,\end{aligned} \quad (19)$$
$$\begin{aligned}&C_i^\top\mathcal{S}_\phi^\top P_{22i}HB_i^\perp + C_i^\top\mathcal{S}_\phi^\top P_{22i}B_i^\top\\&+(B_i^\perp)^\top H^\top P_{22i}^\top\mathcal{S}_\phi C_i + B_iP_{22i}^\top\mathcal{S}_\phi C_i - W_{i\phi} < 0.\end{aligned} \quad (20)$$

The above inequalities imply that (18) holds by setting $S_\phi = V_\phi^{-1}U_\phi$.

2) The regularity and impulse freeness of SMD (9) can be guaranteed by inequalities (15) and (16). Without loss of generality, there exist matrices $A_{11i\phi}$, $A_{12i\phi}$, $A_{21i\phi}$, $A_{22i\phi}$ and invertible matrices $L_{1i\phi}$, $L_{2i\phi}$ such that
$$\begin{aligned}A_{i\phi} &= L_{1i\phi}\begin{bmatrix}A_{11i\phi} & A_{12i\phi}\\ A_{21i\phi} & A_{22i\phi}\end{bmatrix}L_{2i\phi},\\ E_i &= L_{1i\phi}\begin{bmatrix}I & 0\\ 0 & 0\end{bmatrix}L_{2i\phi}.\end{aligned} \quad (21)$$

Then define $\bar{P}_i = L_{1i\phi}^\top P_iL_{2i\phi}^{-1}$ and block the matrix to be compatible with matrix $A_{i\phi}$:
$$\bar{P}_i = \begin{bmatrix}\bar{P}_{11i} & \bar{P}_{12i}\\ \bar{P}_{21i} & \bar{P}_{22i}\end{bmatrix}. \quad (22)$$
Due to the symmetry of the matrix $E_i^\top P_i$ in (16), it can be derived $\bar{P}_{12i} = 0$. Pre- and post-multiplying (15) by $L_{2i\phi}^{-\top}$ and $L_{2i\phi}^{-1}$, respectively, and combining (16) - (22), the following inequality holds
$$\sum_{\phi\in\mathcal{N}}\vartheta_{i\phi}\begin{bmatrix}U_{11i\phi} & U_{12i\phi}\\ * & A_{22i\phi}^\top\bar{P}_{22i} + \bar{P}_{22i}^\top A_{22i\phi}\end{bmatrix} < 0, \quad (23)$$
where matrices $U_{11i\phi}$ and $U_{12i\phi}$ are easy to obtain and irrelevant to the next proof, so omitted here. It can be derived directly from (23) that:
$$\sum_{\phi\in\mathcal{N}}\vartheta_{i\phi}[A_{22i\phi}^\top\bar{P}_{22i} + \bar{P}_{22i}^\top A_{22i\phi}] < 0, \quad (24)$$

which indicates $A_{22i\phi}$ is nonsingular for $i \in \mathcal{M}$, $\phi \in \mathcal{N}$, then the descriptor SMJS (9) is regular and impulse-free.

3) The stochastic stability analysis of the closed-loop system is given. Denote $\mathcal{L}$ as the infinitesimal operator, and the weak infinitesimal generator of $V_1(x(t), r_t, \sigma_t, t)$ is calculated by

$$\begin{aligned}
&\mathcal{L}V_1(x(t), r_t, \sigma_t, t)\\
&= \lim_{\Delta\to 0^+} \frac{1}{\Delta}\mathbb{E}\left[V_1(x(t+\Delta), r_{t+\Delta}, \sigma_{t+\Delta}, t+\Delta\right.\\
&\quad \left.\mid x(t), r_t, \sigma_t, t) - V_1(x(t), r_t, \sigma_t, t)\right]\\
&= \lim_{\Delta\to 0^+} \frac{1}{\Delta}\Bigg[\mathbb{E}\Bigg\{\sum_{j\neq i, j\in\mathcal{M}} \Pr\{R_{k+1}=j, T_{k+1}\leqslant h+\Delta \mid\\
&\quad R_k = i, T_{k+1} > h\}\, x^\top(t+\Delta)E_j^\top P_j x(t+\Delta)\\
&\quad + \Pr\{T_{k+1} > h+\Delta \mid T_{k+1} > h, R_k = i\}\times\\
&\quad x^\top(t+\Delta)E_i^\top P_i x(t+\Delta)\Bigg\} - x^\top(t)E_i^\top P_i x(t)\Bigg]\\
&= \lim_{\Delta\to 0^+} \frac{1}{\Delta}\Bigg[\mathbb{E}\Bigg\{\sum_{j\neq i, j\in\mathcal{M}} \frac{\Pr\{R_{k+1}=j, R_k=i\}}{\Pr\{R_k=i\}}\times\\
&\quad \frac{\Pr\{T_{k+1}\leqslant h+\Delta, T_{k+1} > h | R_{k+1}=j, R_k=i\}}{\Pr\{T_{k+1} > h | R_k = i\}}\times\\
&\quad x^\top(t+\Delta)E_j^\top P_j x(t+\Delta)\\
&\quad + \frac{\Pr\{T_{k+1}\leqslant h | R_{k+1}=i\}}{\Pr\{T_{k+1}\leqslant h | R_k=i\}} x^\top(t+\Delta)P_i x(t+\Delta)\Bigg\}\\
&\quad - x^\top(t)E_i^\top P_i x(t)\Bigg].
\end{aligned} \tag{25}$$

It follows from the general distribution of the mode dwell time and the conditional probability formula that

$$\begin{aligned}
&\mathcal{L}V_1(x(t), r_t, \sigma_t, t)\\
&= \lim_{\Delta\to 0^+} \frac{1}{\Delta}\Bigg[\mathbb{E}\Bigg\{\sum_{j\neq i, j\in\mathcal{M}} q_{ij}\frac{G_i(h+\Delta)-G_i(h)}{1-G_i(h)} x^\top(t+\Delta)\\
&\quad \times E_j^\top P_j x(t+\Delta) + \frac{1-G_i(h+\Delta)}{1-G_i(h)}[x(t+\Delta)-x(t)]^\top\\
&\quad \times E_i^\top P_i x(t+\Delta) + \frac{1-G_i(h+\Delta)}{1-G_i(h)} x^\top(t+\Delta)E_i^\top P_i\\
&\quad \times [x(t+\Delta)-x(t)] - \frac{G_i(h+\Delta)-G_i(h)}{1-G_i(h)}\\
&\quad \times x^\top(t)E_i^\top P_i x(t)\Bigg\}\Bigg].
\end{aligned} \tag{26}$$

Considering the transition rates $\theta_i(h)$ of the system switching from mode i with sufficiently small time period Δ, it yields that

$$\begin{aligned}
&\lim_{\Delta\to 0^+} \frac{1-G_i(h+\Delta)}{1-G_i(h)} = 1,\\
&\lim_{\Delta\to 0^+} \frac{G_i(h+\Delta)-G_i(h)}{1-G_i(h)} = 0,\\
&\lim_{\Delta\to 0^+} \frac{G_i(h+\Delta)-G_i(h)}{\Delta(1-G_i(h))} = \theta_i(h).
\end{aligned} \tag{27}$$

Substituting (27) into (26) gives rise to

$$\begin{aligned}
\mathcal{L}V_1(t) = \ &\mathbb{E}\Bigg\{x^\top(t)\Bigg(\sum_{j\neq i, j\in\mathcal{M}} q_{ij}\theta_i(h)E_j^\top P_j\Bigg)x(t)\\
&+2\sum_{\phi\in\mathcal{N}} \vartheta_{i\phi} x^\top(t)P_iE_i\dot{x}(t)\\
&-\theta_i(h)x^\top(t)E_i^\top P_i x(t)\Bigg\}.
\end{aligned} \tag{28}$$

Recalling transition rates in (3) and $\theta_{ii}(h) = -\sum_{j\neq i, j\in\mathcal{M}} \theta_{ij}(h)$ in (1), it leads to

$$\begin{aligned}
\mathcal{L}V_1(t) \ = \ &\sum_{\phi\in\mathcal{N}} \vartheta_{i\phi} x^\top(t)\left(P_i^\top \bar{A}_{i\phi} + \bar{A}_{i\phi}^\top P_i\right)x(t)\\
&+ \sum_{j\in\mathcal{M}} \bar{\theta}_{ij} x^\top(t)E_j^\top P_j x(t).
\end{aligned} \tag{29}$$

The conditions (15) and (16) guarantee the SA of the system (9). Thus, according to Definition 1, the descriptor SMJS (9) is stochastically admissible. ■

Subsequently, a learning-based SMC law is designed under which the attainability of sliding surface can be ensured, in other words, the system state trajectories are able to approach the sliding manifold steered by the SMLC law.

Theorem 2: For the SMJSs (1) under the synthesized sliding surface function in (5) and the sliding surface parametric matrices S_ϕ obtained in Theorem 1 with $S_\phi, \forall\phi \in \mathcal{N}$, the following SMLC law in (30) solves the reachability problem of sliding surface

$$u(t) = u(t-\ell) + \triangle u(t) \tag{30}$$

with the learning term:

$$\triangle u(t) = \begin{cases} -M_{i\phi}\left(\varrho_1\hat{\dot{V}}(t-\ell) + \varrho_2 V_2(t)\right), & \text{for } s(\phi,t)\neq 0,\\ 0, & \text{for } s(\phi,t) = 0,\end{cases}$$

where $M_{i\phi} = (s^\top(\phi,t)S_\phi C_i B_i)^{-1}$, $V_2(t)$ is a Lyapunov function of sliding surface. Furthermore, $\dot{V}_2(t-\ell)$ is the value of $\mathcal{L}V_2(t)$ at time instant $t-\ell$ and $\hat{\dot{V}}(t-\ell)$ is the numerical approximation of $\dot{V}_2(t-\ell)$:

$$\hat{\dot{V}}(t-\ell) = \frac{V_2(t-3\ell) - 4V_2(t-2\ell) + 3V_2(t-\ell)}{2\ell}. \tag{31}$$

Also, ϱ_1 and ϱ_2 are specified scalars which can be chosen as

$$\frac{1}{\upsilon} < \varrho_1 < 1 - \frac{1}{\upsilon} - \gamma, \quad \varrho_2 > 0, \tag{32}$$

where $\upsilon \in \mathbb{R}_+$ need to satisfy $1 \ll \upsilon$ and $0 < \gamma \ll 1$.

Proof: Construct the Lyapunov function candidate as:

$$V_2(s(\phi,t), r_t, \sigma_t, t) = \frac{1}{2}s^T(\phi,t)s(\phi,t). \tag{33}$$

Replacing $V_2(s(\phi,t), r_t, \sigma_t, t)$ by $V_2(t)$ for simplicity, the weak infinitesimal generator on $V_2(t)$ gives

$$\mathcal{L}V_2(t) = s^\top(\phi,t)S_\phi C_i\left[A_i x(t) + B_i u(t) + B_i f(t, x(t))\right], \tag{34}$$

where ℓ is sufficiently small and $\dot{V}(t,t-\ell)\neq 0$, $\dot{V}_2(t-\ell)\neq 0$ and $\dot{\hat{V}}(t-\ell)\neq 0$. Under acceptable approximation errors, the following Lipschitz-like condition holds

$$\begin{aligned}\left|\dot{V}(t,t-\ell)-\dot{V}_2(t-\ell)\right|&<\frac{1}{\upsilon}\dot{\hat{V}}(t-\ell),\\ \left|\dot{V}_2(t-\ell)-\dot{\hat{V}}(t-\ell)\right|&<\gamma|\dot{\hat{V}}(t-\ell)|,\end{aligned}\tag{35}$$

where

$$\begin{aligned}\dot{V}(t,t-\ell):=&s^\top(\phi,t)S_\phi C_i[A_ix(t)+B_if(t,x(t))\\&+B_iu(t-\ell)].\end{aligned}$$

The following inequalities are satisfied:

$$\begin{aligned}\mathcal{L}V_2(t)=&\dot{V}(t,t-\ell)-\varrho_1\dot{\hat{V}}(t-\ell)-\varrho_2V_2(t)\\ \leqslant&|\dot{V}(t,t-\ell)-\dot{V}_2(t-\ell)|\\&+\dot{V}_2(t-\ell)-\varrho_1\dot{\hat{V}}(t-\ell)-\varrho_2V_2(t)\\ <&\frac{1}{\upsilon}\dot{\hat{V}}(t-\ell)+\dot{V}_2(t-\ell)-\varrho_1\dot{\hat{V}}(t-\ell)-\varrho_2V_2(t).\end{aligned}\tag{36}$$

The numerical solution of three-point numerical differential formula $\dot{\hat{V}}(t-\ell)$ in (31) is used to approximate differential $\dot{V}_2(t-\ell)$, assuming that both symbols are identical. Next, the following reachability analysis can be classified into two different conditions.

Case 1: $\dot{\hat{V}}(t-\ell)>0$ and $\dot{V}_2(t-\ell)>0$, (36) can then be rewritten in this case as

$$\mathcal{L}V_2(t)<\dot{V}_2(t-\ell)+\left(\frac{1}{\upsilon}-\varrho_1\right)\dot{\hat{V}}(t-\ell)-\varrho_2V_2(t).\tag{37}$$

By virtue of (32), inequality (37) can be reformulated as follows

$$\begin{aligned}\mathcal{L}V_2(t)<&\dot{V}_2(t-\ell)-\left|\frac{1}{\upsilon}-\varrho_1\right|\dot{\hat{V}}(t-\ell)-\varrho_2|V_2(t)|\\ <&\dot{V}_2(t-\ell).\end{aligned}\tag{38}$$

Recalling the condition $\dot{V}_2(t-\ell)>0$ and inequality (37), it can be derived that $\dot{V}_2(t)$ continuously decreases with respect to t. There exists an instant t_0 such that $\dot{V}_2(t_0)=0$, one can get when $t=t_0+\ell$

$$\begin{aligned}\mathcal{L}V_2(t_0+\ell)=&\dot{V}(t_0+\ell,t_0)+\varrho_1\dot{\hat{V}}(t_0)-\varrho_2V_2(t_0+\ell)\\ <&\mathcal{L}V_2(t_0)=0.\end{aligned}\tag{39}$$

The above inequality indicates that the value of $\mathcal{L}V_2(t_0)$ can invariably turn from positive to negative. Thus, the condition of $\dot{\hat{V}}(t-\ell)<0$ and $\dot{V}_2(t-\ell)<0$ can be attain by the designed SMLC law.

Case 2: $\dot{\hat{V}}(t-\ell)<0$ and $\dot{V}_2(t-\ell)<0$, from (35), one has

$$\begin{aligned}\dot{V}_2(t-\ell)\;&<\;\dot{\hat{V}}(t-\ell)+\gamma|\dot{\hat{V}}(t-\ell)|\\&<\;(\gamma-1)|\dot{\hat{V}}(t-\ell)|.\end{aligned}\tag{40}$$

Rewriting (27) in this case as

$$\begin{aligned}\mathcal{L}V_2(t)\;&<\;\frac{1}{\upsilon}\dot{\hat{V}}(t-\ell)+(\gamma-1)\left|\dot{\hat{V}}(t-\ell)\right|\\&\quad-\varrho_1\dot{\hat{V}}(t-\ell)-\varrho_2V_2(t)\\&<\;\left(\frac{1}{\upsilon}+\gamma-1+\varrho_1\right)\left|\dot{\hat{V}}(t-\ell)\right|-\varrho_2V_2(t).\end{aligned}\tag{41}$$

It follows from (32) that $\frac{1}{\upsilon}+\gamma-1+\varrho_1<0$, then

$$\begin{aligned}\mathcal{L}V_2(t)\;&<\;-\left|\frac{1}{\upsilon}+\gamma-1+\varrho_1\right|\left|\dot{\hat{V}}(t-\ell)\right|-\varrho_2V_2(t)\\&<\;-\varrho_2V_2(t)<0.\end{aligned}\tag{42}$$

Then, the attainability of sliding mode surface can be achieved, which completes the proof of reachability of sliding mode. ■

Remark 4: Note that the proposed SMLC controller in (30) excludes non-smooth terms, allowing the sliding variable can avoid crossing the sliding surface with a sawtooth wave, thus reducing the switch-related chattering effectively. For iterative learning control law, incorporating a fractional power update rule, as suggested in [39], has the potential to enhance the convergence rate. It is a challenging and promising topic to combine the iterative term in (30) with the fractional order update rate while maintaining the smooth control performance.

IV. Numerical Examples

To demonstrate the effectiveness and potential of the obtained result, practical examples of continuous stirred tank reactor (CSTR) system and F-404 aircraft engine (FAE) system are presented in the section.

A. CSTR System

As schematically depicted in Fig. 1, the CSTR system is a hermetically sealed reaction equipment, in which the reactant concentration and flowrate of the feed have a major impact on the temperature control. According to the reaction mechanism and heat transfer, the mechanism model of reaction temperature and material concentration is established based on the component and energy balance equation:

$$\begin{cases}\dfrac{\mathrm{d}Q_\alpha}{\mathrm{d}t_m}=\dfrac{q_I}{V}(Q_I-Q_\alpha)-C_1Q_\alpha,\\ \dfrac{\mathrm{d}T_\alpha}{\mathrm{d}t_m}=\dfrac{q_I}{V}(T_I-T_\alpha)-\dfrac{H_t}{\rho VQ_p}(T_\alpha-T_c)-\dfrac{C_1(-\Delta T)}{\rho Q_p}Q_\alpha,\end{cases}$$

where Q_α and T_α are concentration and temperature of reactant, respectively. Q_I and T_I are concentration and temperature of feed, respectively. q_I and V are flowrate of feed and volume, respectively. Q_p and T_c are specific heat capacity and coolant temperature, respectively. ΔT and W are reaction heat and activation energy, respectively. H_t and ρ are heat transfer item and density, respectively. $C_1=C_0\exp\left(-\frac{W}{RT}\right)$ with molar gas constant R and C_0 is the reaction rate.

Define the dimensionless state variable as

$$\begin{aligned}x_1(t)\;&=\;\frac{Q_f-Q_\alpha}{Q_\alpha},\\ x_2(t)\;&=\;\frac{T_\alpha-T_I}{T_I}\left(\frac{W}{RT_I}\right),\end{aligned}\tag{43}$$

and dimensionless parameters as

$$\begin{aligned}\mathcal{L}_\alpha\;&=\;\frac{W}{RT_I},\quad\mathcal{B}_\alpha=\frac{Q_\alpha(-\Delta T)}{\rho Q_pT_I}\mathcal{L}_\alpha,\\ \mathcal{D}_\alpha\;&=\;\frac{C_0V\exp(\mathcal{L}_\alpha)}{q_I},\quad b_p=\frac{h_A}{q_I\rho Q_p},\end{aligned}\tag{44}$$

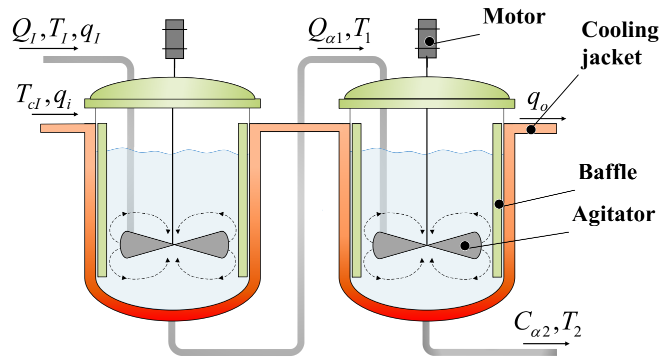

Fig. 1. Schematic of continuous stirred tank reactor.

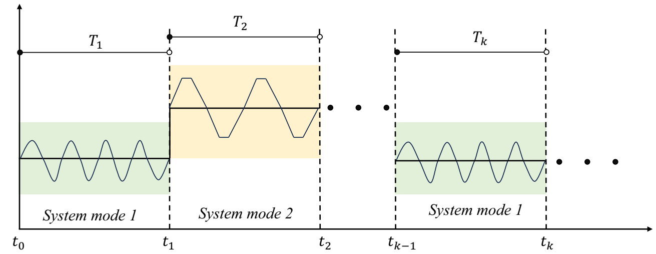

Fig. 2. Illustration of mode switching and state evolution.

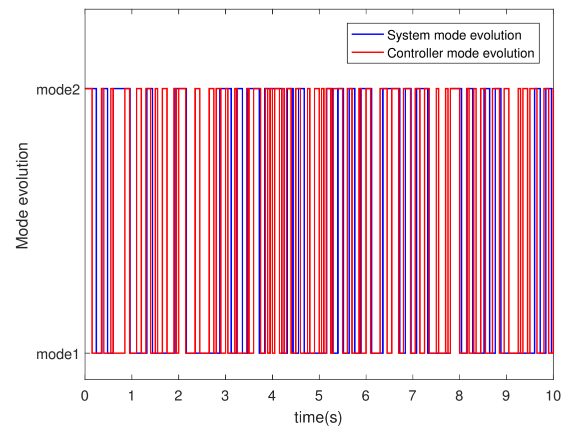

Fig. 3. System and controller mode evolution.

then the dimensionless model of CSTR is described as

$$\begin{aligned}\frac{\mathrm{d}x_1(t)}{\mathrm{d}t}=&-x_1(t)+\mathcal{D}_\alpha(1-x_1(t))\exp\left(\frac{\mathcal{L}_\alpha x_2(t)}{\mathcal{L}_\alpha+x_2(t)}\right),\\ \frac{\mathrm{d}x_2(t)}{\mathrm{d}t}=&-x_2(t)+\mathcal{B}_\alpha\mathcal{D}_\alpha(1-x_1(t))\exp\left(\frac{\mathcal{L}_\alpha x_2(t)}{\mathcal{L}_\alpha+x_2(t)}\right)\\ &+b_p(u(t)-x_2(t)).\end{aligned}\tag{45}$$

During the manufacturing process, changes in external conditions such as raw materials or production conditions would cause sudden shifts or frequent fluctuations in operating conditions. However, despite the stochastic nature of these mode transitions, the system states continuously evolve over time. It demonstrates continuity in transition time accompanied by randomness in mode switching, as shown in Fig. 2. In [40] and [41], the Markov chain is introduced to model the multiple operating conditions of CSTR system. In order to compensate for the limitation of memoryless transition rates and broaden the applicability of stochastic switching systems, the CSTR model with semi-Markov characteristics is inscribed in our previous study [17]. Based on the operating point, the CSTR system can be described as

$$\begin{cases}\dot{x}(t)=\underbrace{\begin{bmatrix}a_{11}(r_t) & a_{12}(r_t)\\ a_{21}(r_t) & a_{22}(r_t)\end{bmatrix}}_{A(r_t)}x(t)+\underbrace{\begin{bmatrix}0\\ b_p\end{bmatrix}}_{B(r_t)}[u(t)+f(t,x(t))]\\ y(t)=C(r_t)x(t),\end{cases}$$

where

$$\begin{aligned}a_{11}(r_t)=&-\mathcal{D}_\alpha\exp\left(\frac{\mathcal{L}_\alpha x_2}{\mathcal{L}_\alpha+x_2}\right)-1,\\ a_{12}(r_t)=&-\mathcal{D}_\alpha\exp\left(\frac{\mathcal{L}_\alpha x_2}{\mathcal{L}_\alpha+x_2}\right)\left(\frac{\mathcal{L}_\alpha x_2}{\mathcal{L}_\alpha+x_2}-\frac{\mathcal{L}_\alpha x_2}{(\mathcal{L}_\alpha+x_2)^2}\right)\\ &(x_1-1),\\ a_{21}(r_t)=&-\mathcal{B}_\alpha\mathcal{D}_\alpha\exp\left(\frac{\mathcal{L}_\alpha x_2}{\mathcal{L}_\alpha+x_2}\right),\\ a_{22}(r_t)=&-\mathcal{B}_\alpha\mathcal{D}_\alpha\exp\left(\frac{\mathcal{L}_\alpha x_2}{\mathcal{L}_\alpha+x_2}\right)\left(\frac{\mathcal{L}_\alpha x_2}{\mathcal{L}_\alpha+x_2}-\frac{\mathcal{L}_\alpha x_2}{(\mathcal{L}_\alpha+x_2)^2}\right)\\ &(x_1-1)-1-b_p.\end{aligned}\tag{46}$$

In this example, the dimensionless parameters are set as $\mathcal{L}_\alpha = 28.5714$, $\mathcal{B}_\alpha = 16.3265$, $\mathcal{D}_\alpha = 0.0281$ and $b_p = 7$. The $x_2(t)$ is measurable variable. The behavior of sojourn-time between different process modes for CSTR system is simulated by Reyleigh distribution and Erlang distribution. For $r_t = 1$, the probability density function and the cumulative distribution function are, respectively, $g_1(h) = \frac{h}{\chi^2}\exp\left(-\frac{h^2}{2\chi^2}\right)$ and $G_1(h) = 1-\exp\left(-\frac{h^2}{2\chi^2}\right)$. For $r_t = 2$, the probability density function and the cumulative distribution function are $g_2(h) = \frac{a^b}{\Gamma(b)}h^{b-1}\exp(-ah)$ and $G_2(h) = 1-\sum_{k=0}^{k-1}\frac{1}{\Gamma(k+1)}\exp(-ah)(ah)^b$, respectively.

Derived from (27), it is easy to get that the transition rate matrix satisfy

$$[\theta(h)] = \begin{bmatrix}-\frac{1}{\chi^2}h & \frac{1}{\chi^2}h\\ \frac{a^b h^{b-1}}{\Gamma(b)\sum\limits_{k=0}^{b-1}\frac{(ah)^k}{\Gamma(k+1)}} & -\frac{a^b h^{b-1}}{\Gamma(b)\sum\limits_{k=0}^{b-1}\frac{(ah)^k}{\Gamma(k+1)}}\end{bmatrix}.\tag{47}$$

Choose the parameters of the sojourn time distribution as $\chi = 0.6\sqrt{2/\pi}$ for $r_t = 1$, $(a, b) = (3, 2)$ for $r_t = 2$. Then, the corresponding the mathematical expectation matrix is

$$[\bar{\theta}_{ij}] = \mathbb{E}[\theta(h)] = \begin{bmatrix}-2.6180 & 2.6180\\ 1.7890 & -1.7890\end{bmatrix},\tag{48}$$

and the emission probability matrix is set by

$$\Upsilon = \begin{bmatrix}0.9 & 0.1\\ 0.2 & 0.8\end{bmatrix}.\tag{49}$$

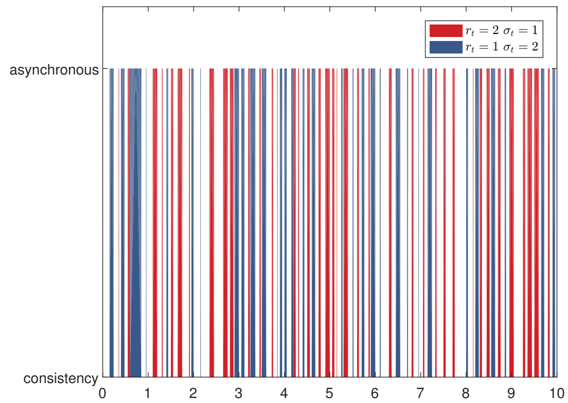

Fig. 4. Asynchronous temporal interval.

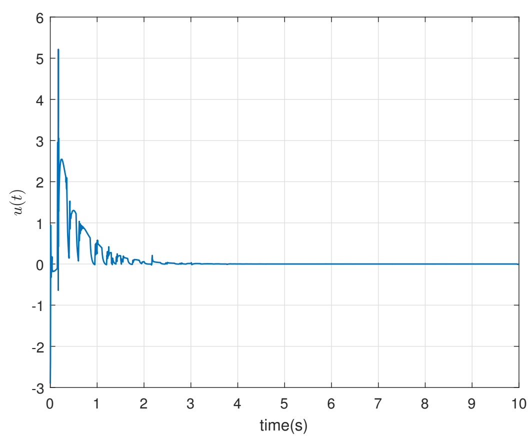

Fig. 5. Control input $u(t)$.

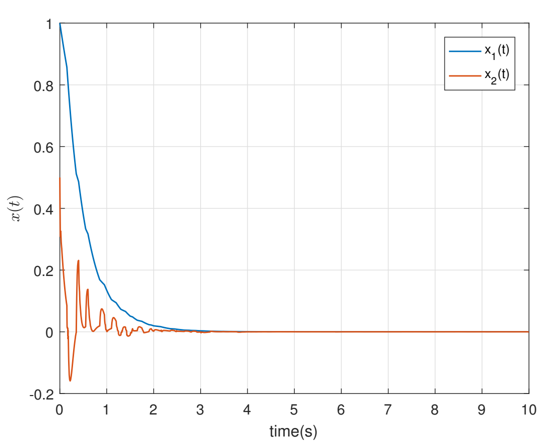

Fig. 6. State response $x(t)$.

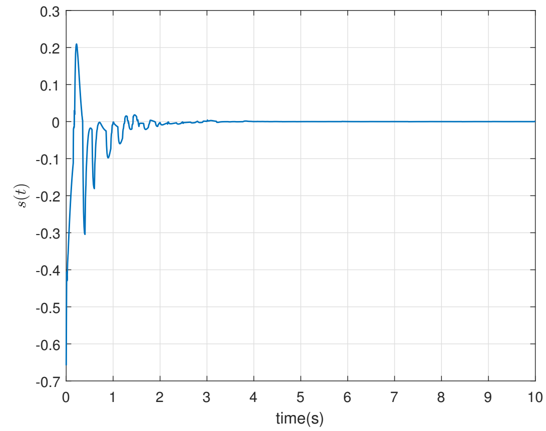

Fig. 7. Sliding surface function $s(\phi, t)$.

Remark 5: For complex systems with multiple operating conditions, for instance, the CSTR system, the asynchrony or disorder of control signals during the transition process may induce disruptive impact in the state variables. The integration of asynchronous control into robust SMC to enhance the control smoothness for multimodal transition systems is of more practical significance.

For the sliding surface design, we can obtain the following sliding surface form Theorem 1:

$$s(\phi, t) = \begin{cases} -1.2987y(t), & \text{for} \quad \sigma_t = 1, \\ -1.3160y(t), & \text{for} \quad \sigma_t = 2. \end{cases} \tag{50}$$

For the SMLC law design, let ϱ_1, ϱ_2 and ℓ be 0.5, 10 and 0.01 in Theorem 2, respectively.

The mode jumping of the CSTR system (45) is governed by the stochastic process r_t, while the mode of controller is determined by the σ_t. Therefore, the modes of the two are not always matched. This phenomenon can be demonstrated by Fig. 3 and asynchronous temporal interval is shown in Fig. 4.

Under the aforementioned SMLC controller shown in Fig. 5, the time evolution of system states and sliding surface are illustrated as Fig. 6 and Fig 7. From the curves of time evolution, the system states and sliding surface function converge to equilibrium point in a finite time. It is clearly shown that the proposed SMLC method can ensure stability and accessibility of global system under the double impact of system modal jump and asynchronous switching.

Remark 6: It is pertinent to note that, in contrast to the stochastic stability criteria obtained in [17] by the construction of the discrete-time semi-Markov kernel, the stochastic stability of the holonomic SMD in this paper is established based on cumulative distribution functions. In addition, for the sake of some inaccessible states of SMJSs, the output-feedback SMC controller design is investigated in this paper. These are two significant differences between this article and the most recent literature [17].

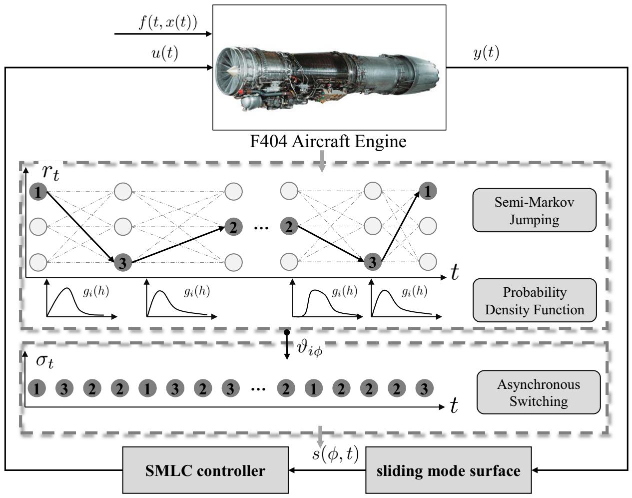

Fig. 8. F404 aircraft engine.

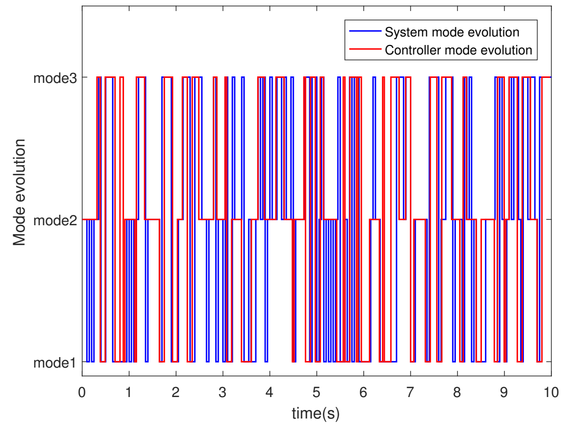

Fig. 9. System and controller mode evolution.

B. FAE System

In this example, the F-404 aircraft engine is used to demonstrate the applicability of the proposed SMLC controller (as shown in Fig. 8) and its model is constructed as follows:

$$\begin{aligned}\dot{x}(t) &= \begin{bmatrix} -1.46 & 0 & 2.428 \\ 0.1643 + 0.5r_t & -1.4 + r_t & -0.3788 \\ 0.3107 & 0 & -2.23 \end{bmatrix} x(t) \\ &\quad + \begin{bmatrix} 0.419 \\ 0.39 \\ 0.519 \end{bmatrix} [u(t) + f(t, x(t))], \\ y(t) &= \begin{bmatrix} 1 & 0 & -1 \\ 0 & 1 & 0 \end{bmatrix} x(t), \end{aligned} \tag{51}$$

where $x(t) = \left[x_1^\top(t)\ x_2^\top(t)\ x_3^\top(t)\right]^\top$, in which $x_1(t)$, $x_2(t)$ and $x_3(t)$ are the sideslip angle, roll rate and the yaw rate, respectively. where the initial condition is given as $x(0) = [1\ 1.5\ -3]^\top$. The nonlinear perturbation function is taken as $f(t, x(t)) = 0.1\sin(t)x_1(t)$. The description of model parameters behavior for $r_t = i \in \{1, 2, 3\}$ utilizes a semi-Markov process. The sojourn time of the semi-Markov chain obeys the Weibull distribution for mode $\overline{1,3}$, of which probability density function from mode i to mode j is $g_i(h) = \frac{b}{a^b} h^{b-1} e^{-(\frac{h}{a})^b}$, where a and b represent the scale parameter and shape parameter of the Weibull distribution, respectively. For $r_t = 1, 3$, the transition rate function $2h$ can be characterized by Weibull distribution with $a = 1$ and $b = 2$; for $r_t = 2$, the transition rate function $3h^2$ can be modeled with $a = 1$ and $b = 3$. The transition rate matrix can be described as follows

$$[\theta(h)] = \begin{bmatrix} -4h & 2h & 2h \\ 3h^2 & -6h^2 & 3h^2 \\ 2h & 2h & -4h \end{bmatrix}. \tag{52}$$

Furthermore, the corresponding mathematical expectation of the transition rate matrix can be derived

$$[\bar{\theta}_{ij}] = \begin{bmatrix} -3.545 & 1.7725 & 1.7725 \\ 2.7082 & -5.4164 & 2.7082 \\ 1.7725 & 1.7725 & -3.545 \end{bmatrix}.$$

The emission probability $\vartheta_{i\phi}$ is listed as

$$[\vartheta_{i\phi}] = \begin{bmatrix} 0.7 & 0.2 & 0.1 \\ 0.2 & 0.7 & 0.1 \\ 0.1 & 0.1 & 0.8 \end{bmatrix}. \tag{53}$$

Especially, the sliding mode parametric matrices can be computed by solving Theorem 1:

$$\begin{aligned} S_1 &= [\ \ 1.58 \quad -21.07\,], \\ S_2 &= [\,-0.01 \quad -17.89\,], \\ S_3 &= [\ \ 2.01 \quad -10.37\,], \end{aligned} \tag{54}$$

let $\varrho_1 = 0.25$, $\varrho_2 = 8$ and $\ell = 0.05$ with the control law (30). Figs. 9-13 showcase the results obtained from the simulation. Fig. 9 depicts the mode switching under probability matrices (52) and (53). Fig. 10 shows the time evolution of FAE state variables (51). It can be seen from the time evolution of states that the system state variables can converge to zero under the proposed SMLC controller in the case of system and controller mode switching and mismatch. Figs. 11 and 12 represent the SMLC input $u(t)$ and the sliding surface function $s(\phi, t)$, respectively. Fig. 13 shows the learning term $\triangle u(t)$. The curves of sliding surface and control input demonstrate that the specific asynchronous sliding surface can be reached and the chattering phenomenon during sliding phase is greatly reduced. Thus, as indicated by the simulation results, effectiveness of the proposed SMLC technique in semi-Markov systems is demonstrated.

V. Conclusions and Future Work

This paper studied the asynchronous SMLC for continuous-time SMJSs via output feedback approach. Based on the dynamical properties of the controlled system and sliding surface, the establishment of a descriptor system allows for the characterization of the holonomic dynamics of the sliding mode. The sufficient conditions of the resultant system stochastic stable are further deduced and the parametric design method of sliding surface is provided. Moreover, a sliding mode learning controller has been designed to drive the underlying global system on the sliding surface. Finally, the resultant approach

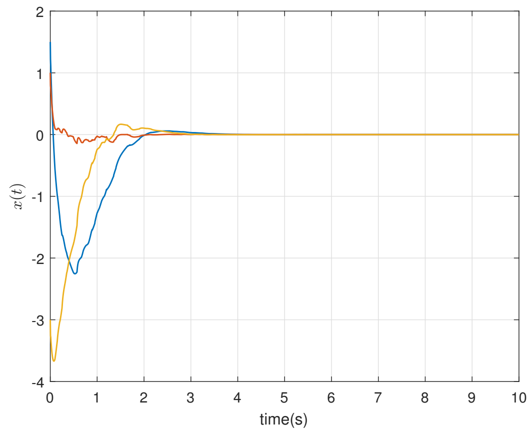

Fig. 10. State response $x(t)$.

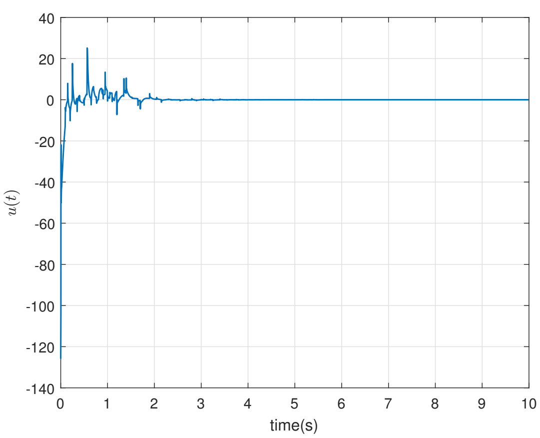

Fig. 11. Control input $u(t)$.

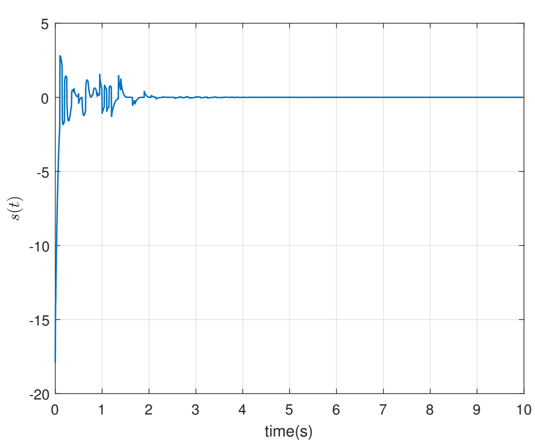

Fig. 12. Sliding surface function $s(\phi, t)$.

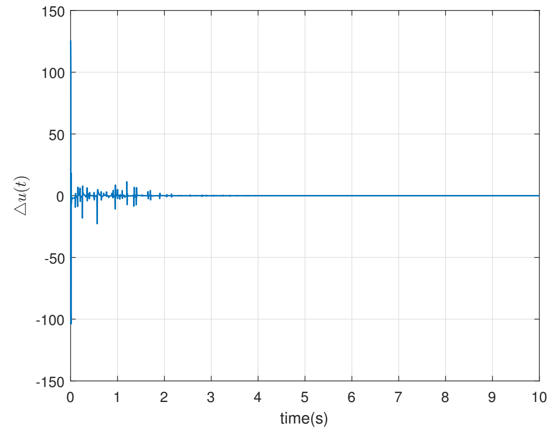

Fig. 13. Learning term $\triangle u(t)$.

is tested and validated through various simulations applied to practical CSTR and FAE models.

The probability density function and emission probability in this article are treated as priori full knowledge. Acquiring complete transition and emission probability is difficult and/or expensive. How to extend the sliding mode-based learning control method to such harsh scenarios without increasing conservatism is worth exploring in the future.

REFERENCES

[1] M. V. Basin, P. Yu and Shtessel, Y. B, “Hypersonic missile adaptive sliding mode control using finite- and fixed-time observers,” *IEEE Trans. Ind. Electrons.*, vol.23, no.1, pp 57–67, 2018.

[2] M. V. Basin, P. C. R. Ramirez and F. Guerra-Avellaneda, ”Continuous fixed-time controller design for mechatronic systems with incomplete measurements,” *IEEE/ASME Trans. Mechatronics*, vol. 23, no. 1, pp. 57–67, 2018.

[3] X. Su, Y. Wen, P. Shi, S. Wang and W. Assawinchaichote, “Event-triggered fuzzy control for nonlinear systems via sliding mode approach,” *IEEE Trans. Fuzzy Syst.*, vol. 29, no. 2, pp. 336–344, 2021.

[4] J. Liu, L. Wu, C. Wu, W. Luo and L. G. Franquelo, “Event-triggering dissipative control of switched stochastic systems via sliding mode,” *Automatica*, vol. 103, pp. 261–273, 2019.

[5] Y. Wei, J. H. Park, J. Qiu, L. Wu and H. Jung, “Sliding mode control for semi-Markovian jump systems via output feedback,” *Automatica*, vol. 21, pp. 133–141, 2017.

[6] L. Wu, J. Liu, S. Vazquez and S. K. Mazumder, “Sliding mode control in power converters and drives: A review,” *IEEE/CAA J. Autom. Sinica.*, vol. 9, no. 3, pp. 392–406, 2022.

[7] J. Li, Y. Niu and J. Song, “Sliding mode control design under multiple nodes round-robin-like protocol and packet length-dependent lossy network,” *Automatica*, vol. 134, article 109942, 2021.

[8] L. Ovalle, H. Ríos, M. Llama and L. Fridman, “Continuous sliding-mode output-feedback control for stabilization of a class of underactuated systems,” *IEEE Trans. Autom. Control*, vol. 67, no. 2, pp. 986–992, 2022.

[9] V. Utkin, “Discussion Aspects of high-order sliding mode control,” *IEEE Trans. Autom. Control*, vol. 61, no. 3, pp. 829–833, 2016.

[10] Y. Liu, H. Li, R. Lu, Z. Zuo and X. Li, “An overview of finite/fixed-time control and its application in engineering systems,” *IEEE/CAA J. Autom. Sinica.*, vol. 9, no. 12, pp. 2106-2120, 2022.

[11] A. Mustafa, N. K. Dhar and N. K. Verma, “Event-triggered sliding mode control for trajectory tracking of nonlinear systems,” *IEEE/CAA J. Autom. Sinica.*, vol. 7, no. 1, pp. 307–314, 2020.

[12] Z. Cao, Y. Niu and C. Peng, “Finite-time stabilization of uncertain Markovian jump systems: an adaptive gain-scheduling control method,” *IEEE Trans. Autom. Control*, DOI: 10.1109/TAC.2023.3307951, 2023.

[13] Z. Zhong, X. Wang and H. K. Lam, "Finite-time fuzzy sliding mode control for nonlinear descriptor systems," *IEEE/CAA J. Autom. Sinica.*, vol. 8, no. 6, pp. 1141–1152, 2021.

[14] A. Rosales, Y. Shtessel, L. Fridman and C. B. Panathula, "Chattering analysis of HOSM controlled systems: frequency domain approach," *IEEE Trans. Autom. Control*, vol. 62, no. 8, pp. 4109–4115, 2017.

[15] M. Liu, L. Zhang, P. Shi and Y. Zhao, "Fault estimation sliding mode observer with digital communication constraints," *IEEE Trans. Autom. Control*, vol. 63, no.10, pp.3434-3441, 2018.

[16] G. P. Incremona, M. Rubagotti, M. Tanelli and A. Ferrara, "A general framework for switched and variable gain higher order sliding mode control," *IEEE Trans. Autom. Control*, vol. 66, no. 4, pp. 1718–1724, 2021.

[17] F. Li, Z. Wu, C. Yang, Y. Shi, T. Huang and W. Gui, "A novel learning-based asynchronous sliding mode control for discrete-time semi-Markov jump systems," *Automatica*, vol. 143, article 110428, 2022.

[18] Z. Man, S. Khoo, X. Yu and J. Jin, "A new sliding mode-based learning control scheme," *2011 6th IEEE Conference on Industrial Electronics and Applications*, pp. 1906-1911, 2011.

[19] D. M. Tuan, Z. Man, C. Zhang and J. Jin, "A new sliding mode-based learning control for uncertain discrete-time systems," *2012 12th International Conference on Control Automation Robotics & Vision (ICARCV)*, pp. 741-746,

[20] X. Hu, C. Hu, X. Si and Y. Zhao, "Robust sliding mode-based learning control for MIMO nonlinear nonminimum phase system in general form," *IEEE Trans. Cybern.*, vol. 49, no. 10, pp. 3793–3805, 2019.

[21] L. Liu, L. Ma, J. Zhang and Y. Bo, "Sliding mode control for nonlinear Markovian jump systems under denial-of-service attacks," *IEEE/CAA J. Autom. Sinica.*, vol. 7, no. 6, pp. 1638–1648, 2020.

[22] O. L. V. Costa, M. D. Fragoso and M. G. Todorov, "A Detector-based approach for the H_2 control of Markov jump linear systems with partial information," *IEEE Trans. Autom. Control*, vol. 60, no. 5, pp. 1219-1234, 2015.

[23] J. Song, Y. Niu and Y. Zou, "Asynchronous sliding mode control of Markovian jump systems with time-varying delays and partly accessible mode detection probabilities," *Automatica*, vol. 93, pp. 33-41, 2018.

[24] X. Su, C. Wang, H. Chang, Y. Yang and W. Assawinchaichote, "Event-triggered sliding mode control of networked control systems with Markovian jump parameters," *Automatica*, vol. 125, Article 109405, 2021.

[25] F. Li, C. Du, C. Yang and W. Gui, "Passivity-based asynchronous sliding mode control for delayed singular Markovian jump systems," *IEEE Trans. Autom. Control*, vol. 63, no. 8, pp. 2715–2721, 2018.

[26] F. Li, C. Du, C. Yang, L. Wu and W. Gui, "Finite-time asynchronous sliding mode control for Markovian jump systems," *Automatica*, vol. 109, Article 108503, 2019.

[27] V. Dragan and E. F. Costa, "Optimal stationary dynamic output-feedback controllers for discrete-time linear systems with Markovian jumping parameters and additive white noise perturbations," *IEEE Trans. Autom. Control*, vol. 61, no. 12, pp. 3912–3924, 2016.

[28] G. Ciardo, R. A. Marie, B. Sericola and K. S. Trivedi, "Performability analysis using semi-Markov reward processes," *IEEE Trans. Comput.*, vol.39, no.10, pp.1251–1264, 2017.

[29] S. Al-Dahidi, F. D. Maio, P. Baraldi and E. Zio, "Remaining useful life estimation in heterogeneous fleets working under variable operating conditions," *Reliab. Eng. Syst. Saf.*, vol. 156, pp. 109–124, 2016.

[30] L. Zhang, T. Yang and P. Colaneri, "Stability and stabilization of semi-Markov jump linear systems with exponentially modulated periodic distributions of sojourn time," *IEEE Trans. Autom. Control*, vol. 62, no. 6, pp. 2870–2885, 2017.

[31] Z. Cao, Y. Niu and Y. Zou, "Adaptive neural sliding mode control for singular semi-Markovian jump systems against actuator attacks," *IEEE Trans. Sys. Man. Cybern. Syst.*, vol. 51, no. 3, pp. 1523–1533, 2021.

[32] J. Huang and Y. Shi, "Stochastic stability and robust stabilization of semi-Markov jump linear systems," *Int. J. Robust. Nonlinear Control*, vol. 23, no. 18, pp. 2028–2043, 2013.

[33] L. Zhang, Y. Leng and P. Colaneri, "Stability and stabilization of discrete-time semi-Markov jump linear systems via semi-Markov kernel approach," *IEEE Trans. Autom. Control*, vol. 61, no. 2, pp. 503–508, 2016.

[34] M. Souza, M. De Almeida, A. R. Fioravanti, and O. L. V. Costa, "$\mathcal{H}_2$ output-feedback cluster control forcontinuous semi-markov jump linear systems with erlang dwell times" *IEEE Control Syst. Lett.*, vol. 7, pp. 109-114, 2023.

[35] Z. Wu, P. Shi, Z. Shu, H. Su and R. Lu, "Passivity-based asynchronous control for Markov jump systems," *IEEE Trans. Autom. Control*, vol. 62, no. 4, pp. 2020–2025, 2017.

[36] B. Saporta and E. F. Costa, "Approximate Kalman-Bucy filter for continuous-time semi-Markov jump linear systems," *IEEE Trans. Autom. Control*, vol. 61, no. 8, pp. 2035–2048, 2016.

[37] J. Zhou, J. H. Park and Q. Kong, "Robust resilient $L_2 - L_\infty$ control for uncertain stochastic systems with multiple time delays via dynamic output feedback," *J. Franklin Inst.*, vol. 353, no. 13, pp. 3078–3103, 2016.

[38] S. Xu and J. Lam, "Robust control and filtering of singular systems," Berlin: Springer, 2006.

[39] Z. Li, D. Shen and X. Yu, "Enhancing iterative learning control with fractional power update law," *IEEE/CAA J. Autom. Sinica.*, vol. 10, no.5, pp. 1137–1149, 2023.

[40] F. Li, X. Cao, C. Zhou, and C. Yang, "Event-triggered asynchronous sliding mode control of CSTR based on Markov model," *J. Franklin Inst.*, vol. 358, pp. 4687–4704, 2021.

[41] M. Fang, H. Kodamana and B. Huang, "Real-time mode diagnosis for processes with multiple operating conditions using switching conditional random fields," *IEEE Trans. Ind. Electron.*, vol. 67, no. 6, pp. 5060-5070, 2020.

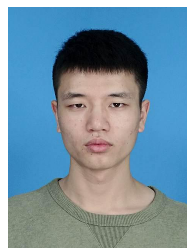

Zheng Wu received the B.S. degree in automation from Hebei University of Technology, Tianjin, China, in 2018, and the M.S. degree in control science and engineering from Central South University, Changsha, China, in 2021. He is now working for a Ph.D. degree in Control Science and Engineering in Central South University, Changsha, China. His research interests include sliding mode control, fuzzy logic systems and semi-Markovian jump systems.

Yiyun Zhao received the B.E. degree in electrical engineering in 2017 from Northwestern Polytechnical University, Xi'an, China, where he is currently working toward the Ph.D. degree with the School of Automation, Northwestern Polytechnical University. His research interests include more electric aircraft, nonlinear control, and mechatronic servo control.

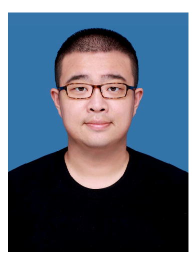

Fanbiao Li (Senior Member, IEEE) received the B.S. degree in applied mathematics from Mudanjiang Normal University, Mudanjiang, China, in 2008, the M.S. degree in operational research and cybernetics from Heilongjiang University, Harbin, China, in 2012, and the Ph.D. degree in control theory and control engineering from the Harbin Institute of Technology, Harbin, in 2015.

From December 2013 to April 2015, he was a Joint Training Ph.D. Student with the School of Electrical and Electronic Engineering, The University of Adelaide, Adelaide, SA, Australia. From April 2015 to February 2016, he was a Research Associate with the School of Electrical and Electronic Engineering, The University of Adelaide. From July 2016 to June 2020, he was an Associate Professor with Central South University, Changsha, China. From April 2017 to March 2018, he was an Alexander von Humboldt Research Fellow with the University of Duisburg–Essen, Duisburg, Germany. He is currently a Full Professor with Central South University. His research interests include control and design of aircraft brake system, sliding-mode control, and fault diagnosis and identification.

Prof. Li currently serves as an Associate Editor for a number of journals, including IEEE Transactions on System, Man, and Cybernetics: Systems, IEEE Transactions on Fuzzy Systems, IEEE/CAA Journal of Automatica Sinica, and Cognitive Computation.

Tao Yang (Senior Member, IEEE) received the M.Eng. degree from Shanghai Jiao Tong University, Shanghai, China, in 2008, and the Ph.D. degree in electrical engineering from the University of Nottingham, Nottingham, U.K., in 2013. Since 2013, he has been a Researcher with the Power Electronics, Machines and Control Group, University of Nottingham, where he became an Assistant Professor in 2016, and an Associate Professor in 2019. His research interests include high-speed electric motor drive control, power electronic conversion, electrical system design, and optimization for more electric/hybrid/all-electric aircraft applications. His Ph.D. research within EU Clean Sky on Modeling electrical power system for more-electric aircraft applications has resulted in him winning the inaugural Clean Sky Best Ph.D. Award in 2016. He is an Associate Editor for the IEEE Transactions on Transportation Electrification and Chinese Journal of Aeronautics.

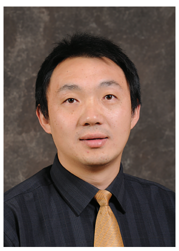

Yang Shi (Fellow, IEEE) received the B.Sc. and Ph.D. degrees in mechanical engineering and automatic control from Northwestern Polytechnical University, Xi'an, China, in 1994 and 1998, respectively, and the Ph.D. degree in electrical and computer engineering from the University of Alberta, Edmonton, AB, Canada, in 2005.

He was a Research Associate with the Department of Automation, Tsinghua University, Beijing, China, from 1998 to 2000. From 2005 to 2009, he was an Assistant Professor and an Associate Professor with the Department of Mechanical Engineering, University of Saskatchewan, Saskatoon, SK, Canada. In 2009, he was with the University of Victoria, Victoria, BC, Canada, and he is currently a Professor with the Department of Mechanical Engineering, University of Victoria. His current research interests include networked and distributed systems, model predictive control, cyber–physical systems, robotics and mechatronics, navigation and control of autonomous systems, and energy system applications.

Dr. Shi was a recipient of the University of Saskatchewan Student Union Teaching Excellence Award in 2007, and the Faculty of Engineering Teaching Excellence Award in 2012 at the University of Victoria (UVic). He is the recipient of the JSPS Invitation Fellowship (short-term) in 2013, the UVic Craigdarroch Silver Medal for Excellence in Research in 2015, the 2017 IEEE Transactions on Fuzzy Systems Outstanding Paper Award, the Humboldt Research Fellowship for Experienced Researchers in 2018; CSME Mechatronics Medal in 2023; and the IEEE Dr.-Ing Eugene Mittelmann Achievement Award in 2023. He is IFAC Council Member; a VP on Conference Activities of IEEE IES and the Chair of IEEE IES Technical Committee on Industrial Cyber-Physical Systems. He is currently a Co-Editor-in-Chief of IEEE Canadian Journal of Electrical and Computer Engineering. He also serves as an Associate Editor for Automatica, IEEE Transactions on Automatic Control, Annual Review in Controls, etc. He is a Distinguished Lecturer of IEEE Industrial Electronics Society. He is a Fellow of ASME, CSME, Engineering Institute of Canada (EIC), Canadian Academy of Engineering (CAE), and a Registered Professional Engineer in British Columbia, Canada.

Weihua Gui (Member, IEEE) received the B.Eng. degree in electrical engineering and the M.Eng. degree in automatic control engineering from Central South University in 1976 and 1981, respectively. From 1986 to 1988 he was a Visiting Scholar at Universität-GH-Duisburg, Germany. Since 1991, he has been a Full Professor at Central South University. Since 2013, he has been an Academician with the Chinese Academy of Engineering. His main research interests include modeling and optimal control of complex industrial process, distributed robust control, and fault diagnoses.